한국동력기계공학회지 제23권 제3호 pp. 18-26 2019년 6월 ISSN 1226-7813(Print) ISSN 2384-1354(Online)
Journal of the Korean Society for Power System Engineering http://dx.doi.org/10.9726/kspse.2019.23.3.018
Vol. 23, No. 3, pp. 18-26, June 2019

Optimum Robust Control for an Oil Cooler System with Variable Speed Drive of Machine Tools

Seok-Kwon Jeong*†

(Received 27 December 2018, Revised 12 February 2019, Accepted 21 February 2019)

Abstract: This paper deals with optimum robust control for an inverter driven oil cooler system of machine tools based on a state space model. An empirical linear first-order model of the oil cooler system obtained by experiments was changed into a state space model suitable for multi-input multi-output optimum controller design. An optimum robust controller was designed to ensure asymptotical stability and robustness against stepwise disturbance and system parameter variation. Effects of two weight matrices in a cost function were observed in detail from experimental results to clarify their trade-off relation. Some experiments were conducted to demonstrate control performance of a designed controller. Experimental results showed that the designed controller had good robustness and fairly good control performance even though abrupt stepwise disturbance addition.

Key Words : Oil Cooler System, Optimum Robust Control, Variable Speed Drive, State Space Model

1. Introduction

Recently, high speed and high precision are required for machine tools to improve their performance. However, the high speed causes unintended deterioration of accuracy and durability of them due to harmful thermal displacement[1]. Therefore, high-precision machine tools need a cooler to eliminate the unnecessary thermal load quickly. Some capacity control techniques for controlling target temperature in the cooler have been applied[1-2]. One approach of the capacity control is a variable speed compressor (VSC) manner. Actually, this manner is more complicated and expensive than hot-gas bypass manner, because it deals with a multi-input and multi-output (MIMO) system and it requires an additional variable speed drive to regulate compressor speed. Nevertheless, it is regarded as an alternative approach in the future because of superior energy saving ability under partial load states, which is highly valued for sustainable development.[1,3-5].

Many different control methods for the VSC such as typical PID[7], PI-feedforward[6-7], linear quadratic regulator (LQR)[8-11], linear quadratic Gaussian (LQG)[12], fuzzy logic[13-14], and artificial neural network have been suggested. Comparing to conventional PID control based on a transfer function model, optimum control based on a state space model has some merits such as flexibility of optimum control design between input energy and control error which are trade-off relation, expendability for the MIMO system, and easiness for securing robustness against modelling error and

*† Seok-Kwon Jeong(ORCID:https://orcid.org/0000-002-9827-4717)
: Professor, Department of Refrigeration and Air-conditioning Engineering, Pukyong National University.
E-mail : skjeong@pknu.ac.kr, Tel : 051-629-6181

disturbances. As the refrigeration cycle included VSC is basically MIMO and high-order nonlinear system, viability for MIMO control and robustness to cope with modelling errors including disturbance are very important factors to accomplish high efficiency and high precision control of the cooler system.

To date, a number of researchers have looked at optimum control of the vapour compression refrigeration system[8-12]. Some of them used LQR[9-11] and another used LQG[12] as a controller. However, robustness of the control system was not fully discussed in the previous studies. Therefore, this paper describes an optimum robust control in a state space model for a cooler included VSC system for machine tools. First of all, we will focus on reference tracking to eliminate steady-state error about stepwise input and robustness against modelling error and disturbance.

At first, a state space model for designing the optimum controller of the cooler was derived from empirical transfer function model obtained experiments. Next, the optimum robust controller was designed based on the state space model to achieve the following control purposes; ① asymptotical stability of control system, ② reference tracking despite stepwise disturbances, ③ robustness against modelling errors. Finally, some experiments were conducted to verify the validity of the suggested controller. Especially, experimental results about the effects of two weight matrices in a cost function are analysed in detail.

2. State Space Model of Oil Cooler System

2.1 Oil cooler system incorporated the VSC

Fig. 1 shows a schematic diagram of a vapour compression refrigeration cycle incorporated VSC and an electronic expansion valve (EEV). Oil outlet temperature of the cooler is the main controlled variable. It is kept as a constant set value for the working of the machine tools by regulating the rotating speed of a compressor using a variable speed drive, an inverter. Superheat in an evaporator is also controlled subsidiarily by an EEV as a constant set value to prevent liquid back phenomenon caused by drastic variation of refrigerant mass flow rate due to sudden change of compressor speed and to operate the system at the condition of maximum coefficient of performance (COP). Hence, the oil cooler system is basically regarded as MIMO system which has two inputs, frequency for an inverter to regulate compressor speed and step for a stepper motor to regulate valve opening angle of an EEV and two outputs, the oil outlet temperature and superheat.

Fig. 2 represents transfer functions between their input and output variables to get an empirical model of the oil cooler system. In here, $G_1(s)$ and $G_4(s)$ are the main transfer functions (TF).

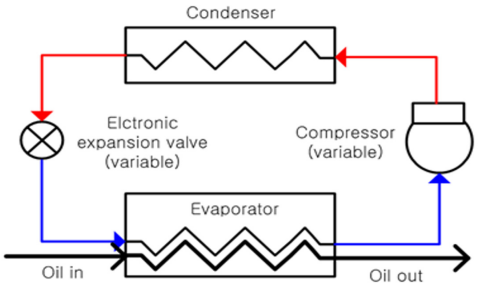

Fig. 1 Schematic diagram of oil cooler system

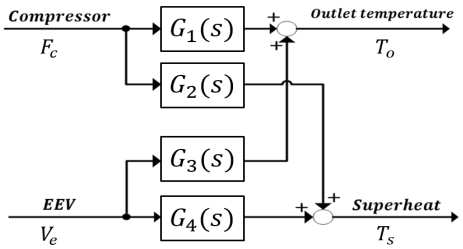

Fig. 2 Input and output variables of TF

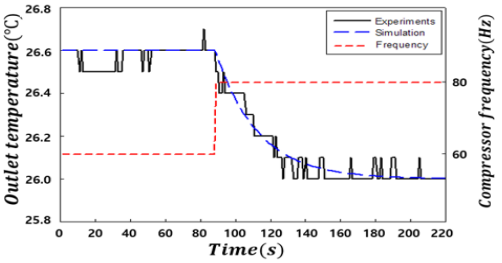

(a) Response of oil outlet temperature

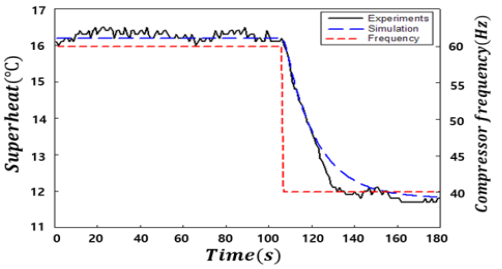

(b) Response of superheat

Fig. 3 Experimental and simulation results of stepwise change in frequency and opening angle

Input variables of the TF are frequency for an inverter and step for a stepper motor, and the corresponding output variables are oil outlet temperature and superheat respectively. On the other hand, $G_2(s)$ and $G_3(s)$ indicate cross-coupling transfer functions which mean interference to each other, and they are ignored in this study because this paper concentrates on the optimum robust controller design.

Fig. 3 shows experimental results to get transfer function models, $G_1(s)$ and $G_4(s)$, and to identify their parameters. Fig. 3 represents responses of oil outlet temperature and superheat when a step input of compressor frequency and valve opening angle were imposed to the oil cooler system. It is noted here that those responses show a typical linear first-order system[8]. Therefore, the transfer function was described as Eq. (1) and their parameters were identified from the experiments.

$$\begin{bmatrix}\delta T_o \\ \delta T_s\end{bmatrix} = \begin{bmatrix}\dfrac{k_{11}}{\tau_{11}s+1} & \dfrac{k_{12}}{\tau_{12}s+1} \\ \dfrac{k_{21}}{\tau_{21}s+1} & \dfrac{k_{22}}{\tau_{22}s+1}\end{bmatrix}\begin{bmatrix}\delta F_c \\ \delta V_e\end{bmatrix} \tag{1}$$

In this equation, symbol 'δ' means amount of variance in temperature and control signal at working point of the system. Also, T_o and T_s are oil outlet temperature and superheat. F_c and V_e represent frequency for a compressor and valve opening angle for an EEV. Identified parameters are as follows; $\tau_{11}=48$, $\tau_{22}=28$, $k_{11}=-0.03$, $k_{22}=-0.018$.

2.2 State space model for an oil cooler

The state space model for an oil cooler system is given as Eq. (2) and Eq. (3) using state variable $X(t)$, input variable $U(t)$, disturbance $D(t)$, and output variable $Y(t)$.

$$\dot{X}(t) = AX(t) + BU(t) + D(t) \tag{2}$$

$$Y(t) = CX(t). \tag{3}$$

Where, $X(t), U(t), Y(t)$ indicate $X(t)=Y(t)=[T_o \;\; T_s]^T$ $U(t)=[F_c \;\; V_e]^T$. Coefficient matrix, A, B, C, were derived as follows:

$$A=\begin{bmatrix}-0.021 & 0 \\ 0 & -0.036\end{bmatrix},\; B=\begin{bmatrix}-0.00063 & 0 \\ 0 & -0.00064\end{bmatrix}$$
$$C=I\;[2\times 2] \tag{4}$$

3. Optimum Robust Controller Design

To achieve the control purposes, an optimum robust control design approach[10-11] is applied. An evaluation function is generally given by Eq. (5).

$$J=\int_0^\infty \{X(t)^T QX(t) + U(t)^T RU(t)\}dt \tag{5}$$

Where, Q and R express weight matrix about state variable and input energy respectively. The main process of this design is divided into two steps. The first step is to choose weight matrix Q and R which is trade-off relation considering the design purpose. The second step is to decide the control input $U(t)$ including state feedback gain matrix K, $U(t) = -KX(t)$, to minimize J and also to be stable closed-loop control system asymptotically.

In servo system, Eq. (5) can not be minimized because the input has $\lim_{t\to\infty} U(t) \neq 0$ even if the output reaches to $\lim_{t\to\infty} Y(t) = R$ in a steady-state. Therefore, a new input $V(t)$, $V(t) = \dot{U}(t)$, was introduced to resolve this problem, then the system equation can be formulated as Eq. (6) and Eq. (7) from Eq. (2) and Eq. (3).

$$\dot{X}_e(t) = A_e X_e(t) + B_e V(t) + D_e D(t) \tag{6}$$

$$Y(t) = C_e X_e(t). \tag{7}$$

Where, $X_e(t) = [X(t) \;\; U(t)]^T$,

$$A_e = \begin{bmatrix} A & B \\ 0 & 0 \end{bmatrix},\; B_e = \begin{bmatrix} 0 \\ I_m \end{bmatrix},\; D_e = \begin{bmatrix} I_n \\ 0 \end{bmatrix},\; C_e = [C \; 0].$$

It is very well known that if the system (A, B) is stable, then the system (A_e, B_e) is also stable. And if (C, A) is observable and rank of Z described Eq. (8) satisfies $Z = n+m$, then the system of (A_e, B_e) is also observable. Here, n means the number of a state variable, m indicates the number of an input of the system. It was confirmed that all of these conditions were fully satisfied from Eq. (4).

$$Z = \begin{bmatrix} A & B \\ C & 0 \end{bmatrix} \tag{8}$$

Considering small variation of the state variable and input variable in a steady-state, $\delta X(t) = X(t) - X_s$, $\delta U(t) = U(t) - U_s$, and let $\delta X_e(t)$ as $\delta X_e(t) = [\delta X(t) \;\; \delta U(t)]^T$, then Eq. (9) and Eq. (10) are derived from Eq. (6) and Eq. (7).

$$\delta \dot{X}_e(t) = A_e \delta X_e(t) + B_e V(t) \tag{9}$$

$$Y(t) - R = C_e \delta X_e(t) \tag{10}$$

Note that the stepwise disturbance $D(t)$ in Eq. (6) was eliminated in Eq. (9) and if the control of $\delta X_e(t)$ converges to 0, then it makes $Y(t) = R$ in Eq. (10). Consequently, the control purpose ② is accomplished by this control. The cost function, Eq. (5) is newly expressed as Eq. (11) using $\delta X_e(t)$, and it can be minimized about J_e.

$$J_e = \int_0^\infty \left\{ \delta X_e(t)^T Q_e \delta X_e(t) + V(t)^T R_e V(t) \right\} dt \tag{11}$$

Here, Q_e is a semi-positive finite symmetric matrix, and R_e is positive finite symmetric matrix. These weight matrices are decided considering control specifications and their maximum limit values. If the weight Q_e is designed as $Q_e = C_e^T C_e$, the weight matrix of energy term, R_e, is only considered in Eq. (11).

The input which is the optimum solution to minimize Eq. (11) can be obtained as follows;

$$V(t) = -K_e \delta X_e(t) \tag{12}$$

$$K_e = R_e^{-1} B_e^T P_e \tag{13}$$

Here, P_e is a positive finite matrix, and it is a solution of the Riccati algebraic equation (14).

$$A_e^T P_e + P_e A_e + Q_e - P_e B_e R_e^{-1} B_e^T P_e = 0 \tag{14}$$

As the values X_s and U_s cannot be known in general, the state feedback of $\delta X_e(t)$ in Eq. (12) is

impossible in reality. Therefore, $\delta X_e(t)$ is replaced by terms of state variable $X(t)$ and control error $Y_e(t) = R - Y(t)$ as Eq. (15) by substituting the definition of $\delta X_e(t)$ to Eq. (12).

$$V(t) = -K_e Z^{-1}\begin{bmatrix} \dot{X}(t) \\ Y(t) - R \end{bmatrix} \tag{15}$$

Here, the term of $K_e Z^{-1}$ means a control gain matrix K. Finally, a control input $U(t)$ is given as;

$$U(t) = -K_1 X(t) + K_2 \int_0^t Y_e(\tau) d\tau + K_1 X(0) \tag{16}$$

Eq. (17) shows augmented matrices A_e, B_e, and C_e.

$$A_e = \begin{bmatrix} -0.021 & 0 & -0.00063 & 0 \\ 0 & -0.036 & 0 & -0.00064 \\ 0 & 0 & 0 & 0 \\ 0 & 0 & 0 & 0 \end{bmatrix},$$

$$B_e = \begin{bmatrix} 0 & 0 \\ 0 & 0 \\ 1 & 0 \\ 0 & 1 \end{bmatrix}, \quad C_e = \begin{bmatrix} 1 & 0 & 0 & 0 \\ 0 & 1 & 0 & 0 \end{bmatrix} \tag{17}$$

Eq. (18) gives weight matrices Q_e and R_e. Thus, controller gain K is calculated as Eq. (19).

$$Q_e = \begin{bmatrix} 1 & 0 & 0 & 0 \\ 0 & 1 & 0 & 0 \\ 0 & 0 & 0 & 0 \\ 0 & 0 & 0 & 0 \end{bmatrix}, \quad R_e = \begin{bmatrix} 1 & 0 \\ 0 & 1 \end{bmatrix} \tag{18}$$

$$K = \begin{bmatrix} -32.132 & 0 & -1 & 0 \\ 0 & -23.054 & 0 & -1 \end{bmatrix} \tag{19}$$

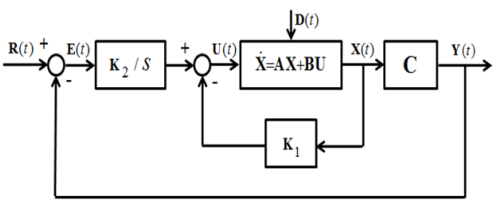

Fig. 4 Optimum robust servo control system

Fig. 4 illustrates the optimum robust control system to realize control law of Eq. (16) under an initial condition of $X(0) = 0$.

4. Experiments and Results

4.1 Experimental device and method

Fig. 5 shows an experimental system for the suggested optimum robust control. A LabVIEW system was used as the control device. Final outputs of this device are analogue voltages corresponding frequency and step for an inverter of a compressor and for a stepper motor drive of an EEV respectively.

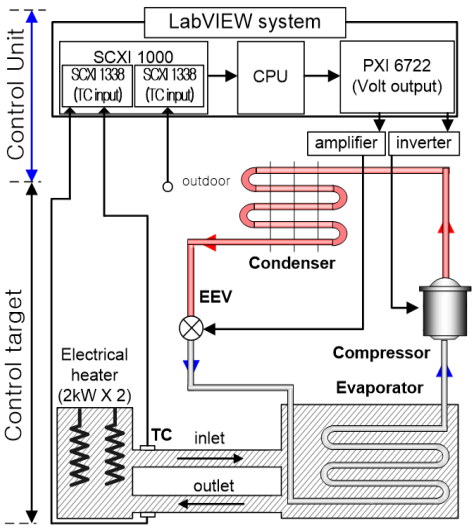

Fig. 5 Experimental system

Table 1 Specifications of the test unit

Component	Note
Compressor	Rotary type, 0.75 ㎾
EEV	Stepping motor type
Heater	4(2×2) ㎾
Refrigerant	R-22
Oil	Mobil velocity No. 3

Table 2 Experimental conditions

Item	Note
Compressor variable range	40~90 Hz
EEV variable range	100~500 step
Oil flow rate	22.5 l/min
Ambient air temperature	30℃
Control period	1 sec

The set point of outlet temperature was 25℃ from real control specification of machine tools, and the set point of superheat was set at 9℃considering maximum COP analysis from a static experimental result.

The scroll type compressor with an induction motor installed inside was driven by a V/f=constant type inverter(0~90 Hz). A stepping motor driven by an exclusive drive controls the opening angle of the EEV(500 steps). Thermocouples were attached at the surface of pipe of inlet and outlet of an evaporator for measuring T_o and T_s.

Table 1 and Table 2 show design specifications of the test unit and experimental conditions.

A static experiment was conducted to confirm suitable superheat reference before dynamic experiments, and appropriate superheat reference, 9℃, was found from the relationship between COP and superheat. Then, three types of dynamic experiments, starting up, thermal load change, and reference change were performed to confirm control performance of the proposed control system. In the starting up experiment, a reference temperature of 25℃ was given as a set value. In the reference change experiment, initial set value of temperature 25℃ was suddenly changed to 24℃ at 100 seconds. In the thermal load change experiment, the reference value of heat load was abruptly changed from 1.2 kW to 1.5 kW under a steady-state.

To investigate effects of two weight matrices in a cost function, two kinds of experiments were performed with respect to the relative magnitude ratio between Q_e and R_e. Also, robustness of the system against parameter variation is discussed through experimental results.

4.2 Experimental results and discussion

Fig. 6 represents the dynamic behaviour of oil outlet temperature in the cases of starting up, reference change, and thermal load change respectively. The experimental results show that the designed controller can keep their set values very precisely within ±0.1℃ error range in steady-state for oil outlet in spite of working condition changes. And the superheat had control accuracy with ±1.5℃ in the same condition as T_o. Furthermore, their corresponding control signals are reasonable within their working range.

Fig. 7 gives dynamic behaviours of oil outlet temperature and corresponding their energy consumption with respect to different combinations of two weight matrices, Q_e and R_e.

Comparing the case of $Q_e : R_e = 1:10$ with $Q_e : R_e = 10:1$, the transient responses of the former was worse than those of the latter because of limited power caused by the big weight of energy term.

As a result, energy consumption was shown as smaller than the latter in natural. In the case of $Q_e : R_e = 10:1$, settling time of control variable was shorter than the case of $Q_e : R_e = 1:1$ and $Q_e : R_e = 1:10$ because of the large weight of control error term, while energy consumption became large during transient time.

Fig. 8 shows dynamic behaviour of oil outlet temperature and its control signal under different ambient temperature from the condition which was taken at initial dynamic model in Eq. (4).

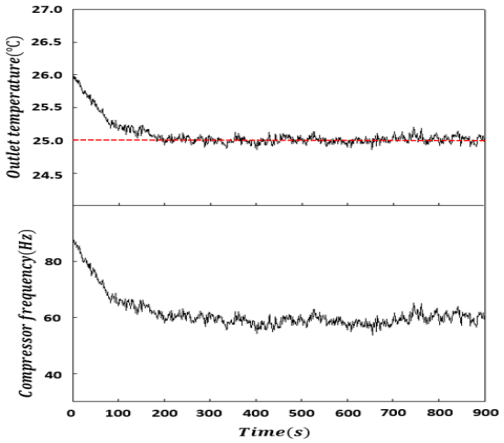

(a) Starting up

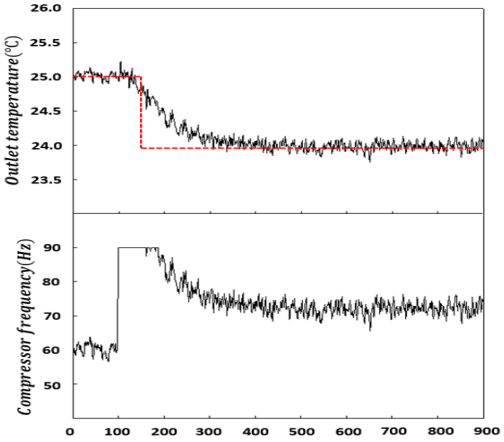

(b) Reference change

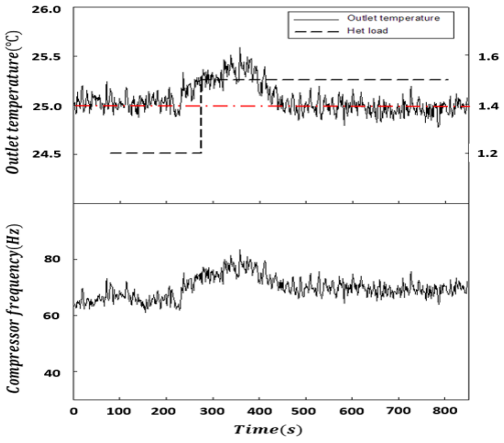

(c) Thermal load change

Fig. 6 Experimental results of T_o and its control signal in the case of $Q_e : R_e = 1 : 1$

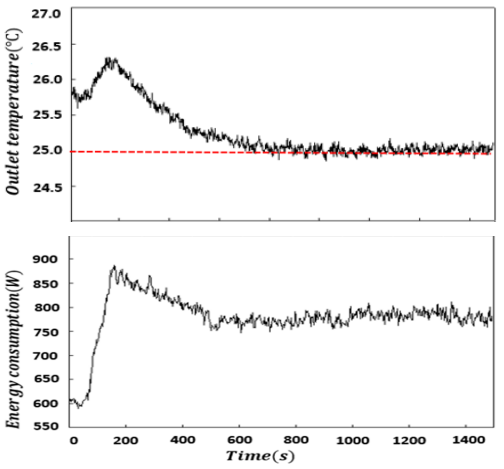

(a) $Q_e : R_e = 1 : 10$

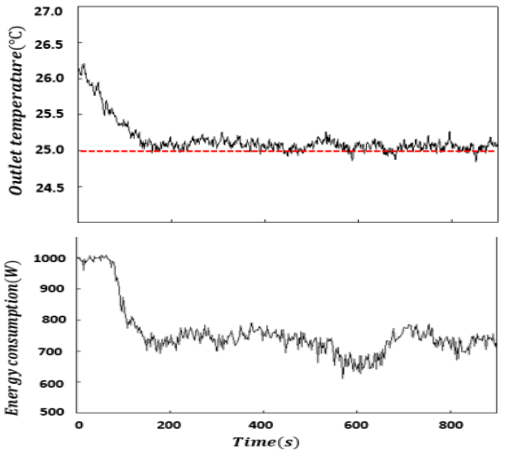

(b) $Q_e : R_e = 10 : 1$

Fig. 7 Experimental results of oil outlet temperature and energy consumption

From these results, it was found that the proposed method had robustness under model uncertainty. Also, the further validation of robustness against small parameter variation about A and B were also verified through computer simulation. The simulation results had robustness against parameter variation of A and B with 30%.

The suggested control method had good robustness even under change in thermal load, ambient temperature T_a, and parameter variation of A and B.

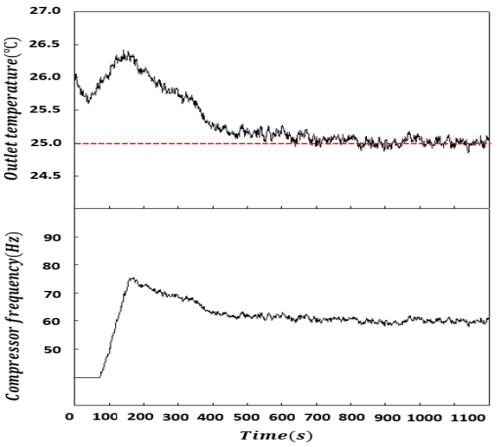

(a) $T_a = 30℃$

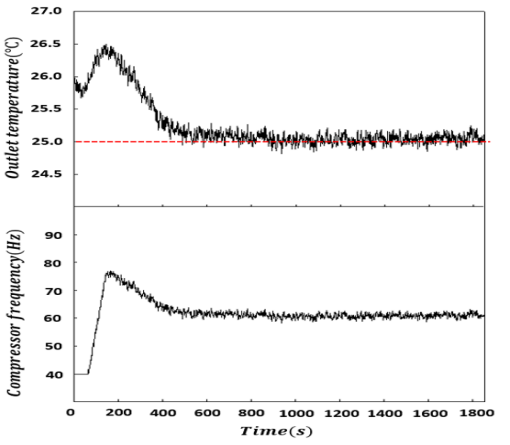

(b) $T_a = 20℃$

Fig. 8 Experimental results of T_o and its signal under different ambient temperature T_a

5. Conclusions

The optimum robust control based on a state space model obtained empirical transfer function model was investigated to control target temperature and superheat simultaneously for an oilcooler system in machine tools. The servo system augmented from a basic state space model was utilized to cope with stepwise reference tracking and to reject stepwise disturbance.

The robustness of the control system against parameter variations was confirmed through some real experiments and computer simulations considering some modelling errors and external disturbances such as change of thermal load and ambient temperature. Especially, the effect of two weight matrices in a cost function was analysed in detail using experimental data to clarify their trade-off relation. The experimental results showed that the suggested robust optimum controller had fairly good control performances such as ±0.1℃ and ±1.5℃ error range in steady-state for oil outlet and superheat respectively in spite of working condition changes. Consequently, it was clear that the optimum robust control can achieve precise reference tracking about stepwise reference despite external disturbances and model errors, and optimum control performances between energy consumption and control errors.

Acknowledgement

This work was supported by a Research Grant of Pukyong National University (2017 year).

References

1. S. K. Jeong, D. B. Lee and K. H. Hong, 2014, "Comparison of system performance on hot-gas bypass and variable speed compressor in an oil cooler for machine tools", Journal of Mechanical Science and Technology, Vol. 28, No. 2, pp. 721-727. (DOI:101007/sl12206-013-1136-1)
2. M. Yaqub, S. M. Zubair and J. U. R Khan, 2000, "Performance evaluation of hot-gas bypass capacity control scheme for refrigeration and air-conditioning systems", Energy, Vol. 25, pp. 543-561.
3. T. N. Aynur, 2010, “Variable refrigerant flow systems: A review”, 2010, Energy and Buildings, Vol. 42, pp. 1106-1112. (DOI:10.1016/j.enbuld.2010.01.024)

4. T. Q. Qureshi and S. A. Tassou, 1996, "Variable-speed capacity control in refrigeration systems", Applied Thermal Engineering, Vol. 16, pp. 103-113.
5. I. H. Lee, J. W. Choi and M. S. Kim, 2011, "Studies on the heating capacity control of a multi-type heat pump system applying a multi-input multi-output (MIMO) method", International Journal of Refrigeration, Vol. 34, pp. 416-428.
6. H. Li, S. K. Jeong and S. S. You, 2009, "Feedforward control of capacity and superheat for a variable speed refrigeration system", Applied Thermal Engineering, Vol. 29, pp. 1067-1074. (DOI:10.1016/j.applthermaleng.2008.05.022)
7. H. Li, S. S. You, J. I. Yoon and S. K. Jeong, 2008, "An empirical model for independent control of variable speed refrigeration system", Applied Thermal Engineering", Vol. 28, pp. 1918-1924. (DOI:10.1016/j.applthermaleng.2007.12.008)
8. J. L. Lin and T. J. Yeh, 2007, "Identification and control of multi-evaporator air-conditioning systems", International Journal of Refrigeration, Vol. 30, pp. 1374-1385. (DOI:10.1016/j.ijrefrig.2007.04.003)
9. R. Shah, A. G. Alleyne and C. W. Bullard, 2004, "Dynamic modelling and control of multi-evaporator air-conditioning systems", ASHREA Transactions, Vol. 110, pp. 109-119.
10. S. H. Kim and S. K. Jeong, 2011, "Optimum controller design of a water cooler for machine tools based on the state space model", KJACR, Vol. 23, No. 12, pp. 782-790.
11. D. B. Lee, S. K. Jeong and Y. M. Jung, 2014, "State equation modelling and the optimum control of a variable-speed refrigeration system", KJACR, Vol. 26, No. 12, pp. 579-587. (DOI:10.6110/KJACR.2014.26.12.579)
12. L. C. Schurt, C. J. L. Hermes and A. T. Neto, 2010, "Assessment of the controlling envelope of a model-based multivariable controller for vapour compression refrigeration systems", Applied Thermal Engineering, Vol. 30, pp. 1538-1546.
13. S. K. Jeong, C. H. Han, H. Li and W. K. Wibowo, 2018, "Systematic design of membership functions for fuzzy logic control of variable speed refrigeration system", Applied Thermal Engineering, Vol. 142, pp. 303-310. (DOI:10.1016/j.applthermaleng.2018.06.082)
14. J. P. Cao, S. K. Jeong and Y. M. Jung, 2014, "Fuzzy logic controller design with unevenly-distributed membership function for high performance chamber cooling system", J. Cent. South Univ., Vol. 21, pp. 2684-2692. (DOI:10.1007/s11771-014-2230-y)